17th World Conference on Earthquake Engineering, 17WCEE
Sendai, Japan - September 13th to 18th 2020

GENERATION OF ENERGY SPECTRUMS USING A SET OF PERUVIAN SEISMIC RECORDS OF ACCELERATIONS

M. Choquehuanca [(1)], J. Avendano [(2)], Victor I. Fernandez-Davila[(3)]

(1) Graduate Student, Pontificia Universidad Católica del Perú, marianella.choquehuanca@pucp.pe
(2) Research Engineer, MSc, Pontificia Universidad Católica del Perú, jenny.avendano@pucp.pe
(3) Associate Professor, Facultad de Ciencias e Ingeniería, Sección de Ingeniería Civil, Pontificia Universidad Católica del Perú, vfernandezdavila@pucp. edu.pe

Abstract

Based on the energy balance equation developed by Housner and Akiyama [1], and using seismic accelerations records measured in Peru a set of energy spectra was generated. These energy spectra allowed to verify that the energy demanded by a severe seismic event is less than the energy dissipation capacity of a structure, which increases the probability of meeting the objectives of structural performance and satisfying with the expected damage control. The energy spectra were generated based on the non-linear seismic response for discrete systems of one degree of freedom, considering that the relevant response is mainly determined by the energy dissipation capacity and, consequently, by the change in the period of vibration. Therefore, to carry out this study, a set of seismic acceleration records and the methodology proposed for Avendaño and Fernandez-Davila [2] were taken as a basis.

The input data consisted of an amount of 68 pairs of seismic acceleration records and were classified and filtered according to Peruvian seismic code E-030 [3], and they are following: Hard Rock (51), Rocky or Rigid Soils (10), Intermediate Soils (9). Besides, from the lateral displacement curves, it was observed that the seismic performance and the response of buildings subjected to severe seismic events were strongly influenced by the geotechnical characteristics in situ and the seismic ground motions.

The main conclusions were: i) Show the shape and the trend of the inelastic spectrum made in base of Peruvian seismic records, ii) Show the importance of the ductility demanded in the application of the methodology proposed herein, since this is a parameter that depend mainly of the lateral resistance and lateral displacement relationship, and therefore, this is a key factor to link the expected nonlinear behavior and the structural response before a large number of seismic events, iii) it was verified that the input energy spectra and the hysterical energy calculation reveal and apply relevant information, such as the total frequency content and duration of the earthquake which are not considered by the typical pseudo-acceleration response spectrum.

Keywords: Balance of Energy; Energy Spectra; Ductility; Hysteretic dissipation; damage control.

1. Introduction

The parameters resulting from the energy response spectra can be used to characterize the seismic events so it is true that the current trend of the resistant earthquake design is to establish the mechanical characteristics required by the structure, so that the damage produced by the dissipation of the plastic energy is consistent with the acceptable level of projected structural damage. One of the most critical aspects of the design review is to determine whether the cumulative deformation capacity and actual maximum deformation is consistent according to the design parameters. On the other hand, knowing the amount of plastic energy dissipated by systems of one degree of freedom is a determining fact to characterize non-linear behavior.

Currently, the structural design methodology is based on performance and considers the inelastic response of the structures, but this methodology does not reveal the hysterical behavior of a structure, which implies a cyclic loading and unloading behavior with a recovery force that It is based on the materials and the different types of structuring. That is why, it is necessary to use energy concepts with which energy demand spectra can be generated (input energy and hysterical energy), which take into account structural properties, site conditions, earthquake intensity and the expected structural ductility, in order to establish reasonable approximations of inelastic energy demands [4].

2. Methodology

Inelastic response spectra were generated for systems of a degree of freedom, based on the expressions of energy balance proposed by Housner and Akiyama [1]. In the case of elastic spectra, the input energy spectrum was first calculated based on Eq (1) to (6) derived from the differential equation of motion:

$$m\ddot{y} + c\dot{y} + Q(y) = -m\ddot{Z}_g \tag{1}$$

$$m\int_0^t \ddot{y}\,\dot{y}dt + c\int_0^t \dot{y}^2\,dt + \int_0^t Q(y)\dot{y}\,dt = -\int_0^t m\ddot{z}_g\dot{y}dt \tag{2}$$

$E_k(t) = m\int_0^t \ddot{y}\,\dot{y}dt = \frac{m\dot{y}^2(t)}{2}$ Kinetic or elastic vibration energy (3)

$E_\xi(t) = c\int_0^t \dot{y}^2 dt$ Energy dissipated by damping (4)

$E_a(t) = \int_0^t Q(y)\,\dot{y}dt$ Energy dissipated by hysteretic deformation (5)

$E_I(t) = -\int_0^t m\ddot{z}_g\dot{y}\,dt$ Input Energy (6)

The Eq. (6) can be expressed as follows:

$$E_k + E_\xi + E_a = E_I \tag{7}$$

The Input Energy (Eq. (7)), is the energy introduced into a structural system at the instant 't' due to the action of the seismic movement. This energy is equivalent to the sum of the kinetic energy, the energy dissipated by the damping and the hysteretic energy. In addition, being a seismic-resistant design tool, it is a stable parameter in the structural response during a seismic event and has little dependence on the properties of the structure.

On the one hand, the hysterical energy is part of the energy input that contributes to structural damage, since it is dissipated by plastic deformation. This energy in terms of quantification, is equal to the total area enclosed by each of the hysteresis cycles developed by the structure during a seismic excitation.
For the elaboration of the input energy response spectra, the energy for a domain of 1000 vibration period values in the range of 0.001s to 4s was calculated. The calculated energy was expressed in units of 'equivalent speed V_E' (representing the energy per unit mass) according to Eq. (8) and the Akiyama methodology [1].

$$V_E = \sqrt{\left(\frac{2E_I}{M}\right)} \quad (8)$$

Where: V_E is the equivalent speed, E_I is the input energy and M is the mass of the system.

2.1. Inelastic and hysterical spectra

Inelastic spectra were generated for systems with a degree of freedom of reinforced concrete (critical damping ratio ξ=5%), using the material behavior model that belongs to the elastoplastic perfect model behavior for structures.
Likewise, the concept of objective ductility according to Bojorquez [5] was applied, setting this value to μ=4 and also the maximum ductile capacity value in monophonic load was used in μ_D= 6 (reasonable for reinforced concrete structures). On the other hand, the Park and Ang damage index was included, according to it, the level of structural damage in reinforced concrete elements and structures subject to cyclic loads can be estimated from the maximum and accumulated demands of plastic deformation and β which is a parameter that depends on the structural characteristics and that characterizes the stability of the hysteretic cycle according to Bojorquez [5]. Thus, for the present work the value of β= 0.15 was used as a parameter of stability of loading and unloading cycles. The Degtra program [6] was used as a computational tool for the elaboration of the spectra. And the SismoSignal program [7] was used for the treatment of seismic records of soil movement.

2.2. Record filter process.
The seismic record filtering process was performed based on soil movement data obtained through the SismoSignal program [7]. The most relevant filter, in addition to the control of frequencies and baseline, was the discrimination of events on an impulsive basis, using the Impulsivity index I_p [8], in this way, records of seismic accelerations with an Ip $I_p \leq 20$ were excluded.

3. Seismic acceleration records

A set of 170 pairs of seismic records of accelerations obtained from CISMID (Japanese Center for Seismic Research and Disaster Prevention) and the IGP (Geophysical Institute of Peru) were filtered, of which 68 non-impulsive seismic records were obtained. Subsequently, with the predominant vibration period parameter, it was possible to perform the soil classification according to what is established in the Peruvian Technical Standar Code E.030 for Seismic Resistant Design of the National Building Regulations (Table 1).

Table 1: Soil Profile according to E.030 Seismic Resistant Design Standard [3]

Periods "T_P" y "T_L"				
	Soil Profile			
	S_0	**S_1**	**S_2**	**S_3**
T_P	0.3	0.4	0.6	1.0
T_L	3.0	2.5	2.0	1.6

Table 2 shows the accelerograms based on which the spectra were made. This table shows the predominant period, the classification according to the soil profile and the calculated impulsivity index. Likewise, seismic registers that are part of the group of accelerograms are included, based on which the acceleration spectrum of the current earthquake-resistant design standard has been developed.

Table 2: Summary chart of accelerograms

N° REG	Name	Station	Date	Period	Intensity Index	Condition	Soil Type E.030	Soil Condition (Table 1)
1	ALTO AMAZ 9E7E 2019	CIP LIMA	22/02/2019	0,291	2582,212	Not impulsive	S0	Hard rock
2	PRQUE RESERVA 1966	PARQUE DE LA RESERVA	17/10/1966	0,128	97,493	Not impulsive	S0	Hard rock
3	PRQ-7005311523	PQR	31/05/1970	0,242	179,065	Not impulsive	S0	Hard rock
4	PRQ-7410030921	PARQUE DE LA RESERVA	03/10/1974	0,323	152,470	Not impulsive	S1	Rigid soils
5	ALTO AMAZ MALA B863	MALA	22/02/2019	0,550	3206,128	Not impulsive	S2	Intermediate soils
6	César Vizcarra MOQ001	ROLANDO CATACORA	13/06/2005	0,323	271,228	Not impulsive	S1	Rigid soils
7	MOL_0708151840	LA MOLINA	15/08/2007	0,184	17,469	Not impulsive	S0	Hard rock
8	TACNA	TACNA	06/05/2010	0,272	93,987	Not impulsive	S0	Hard rock
9	PASTAZA 2019-BDC9	ANCASH SANTA	22/02/2019	0,072	725,636	Not impulsive	S0	Hard rock
10	PASTAZA AMAZONAS C23	ANCASH SANTA	22/02/2019	0,184	1082,483	Not impulsive	S0	Hard rock
11	PASTAZA C163	ANCASH SANTA	22/02/2019	0,241	1104,927	Not impulsive	S0	Hard rock
12	PURUS BDC9	ANCASH SANTA	05/01/2019	0,085	4875,302	Not impulsive	S0	Hard rock
13	PURUS C23E	ANCASH SANTA	05/01/2019	0,198	4680,131	Not impulsive	S0	Hard rock
14	AZANGARO C16B	TACNA CALANA	01/03/2019	0,226	1004,709	Not impulsive	S0	Hard rock
15	AZANGARO C166	CIP AQP	01/03/2019	0,206	970,355	Not impulsive	S0	Hard rock
16	AZANGARO C189	ALTO DE LA ALIANZA	01/03/2019	0,184	579,238	Not impulsive	S0	Hard rock
17	AZANGARO D8CF	CIP AREQUIPA 2	01/03/2019	0,156	915,566	Not impulsive	S0	Hard rock
18	PURUS UCAYALI BDC9	ANCASH SANTA	24/08/2018	0,100	8455,684	Not impulsive	S0	Hard rock
19	LOMAS B863	MALA	14/01/2018	0,501	637,773	Not impulsive	S2	Intermediate soils
20	LOMAS AREQUIPA D859	PALPA	14/01/2018	0,215	234,939	Not impulsive	S0	Hard rock
21	ZARUMILLA TUMBES BDBF	UNAB BARRANCA	06/09/2018	0,072	11929,284	Not impulsive	S0	Hard rock
22	TARATA TACNA B859	PALPA	15/03/2019	0,457	2518,727	Not impulsive	S2	Intermediate soils
23	TARATA TACNA C16B	CIP TACNA	15/03/2019	0,241	1394,893	Not impulsive	S0	Hard rock
24	TARATA TACNA D8CE	CIP PISCO	15/03/2019	0,161	19990,836	Not impulsive	S0	Hard rock
25	TARATA TACNA C189	ALTO DE LA ALIANZA	15/03/2019	0,170	1101,258	Not impulsive	S0	Hard rock
26	TACNA C166	JLBR AREQUIPA	01/11/2018	0,141	1797,820	Not impulsive	S0	Hard rock
27	TACNA C189	ALTO DE LA ALIANZA	01/11/2018	0,233	648,987	Not impulsive	S0	Hard rock
28	TACNA D859	PALPA	01/11/2018	0,113	9527,478	Not impulsive	S0	Hard rock
29	TACNA C16B	CIP TACNA	10/10/2017	0,269	294,841	Not impulsive	S0	Hard rock
30	TACNA C166	CIP AQP	10/10/2017	0,226	502,189	Not impulsive	S0	Hard rock
31	MANCORA PIURA C164	PIURA	05/06/2017	0,243	651,884	Not impulsive	S0	Hard rock
32	LA MERCED C17A	CIP HUANUCO	13/08/2017	0,311	513,026	Not impulsive	S1	Rigid soils
33	PALPA ICA 9E7E	CIP LIMA	24/01/2019	0,200	5239,085	Not impulsive	S0	Hard rock
34	PALPA ICA B863	MALA	24/01/2019	0,113	1089,899	Not impulsive	S0	Hard rock
35	PALPA ICA BDBF	UNAB BARRANCA	24/01/2019	0,400	6641,557	Not impulsive	S1	Rigid soils
36	PALPA ICA C1EA	TACNA	24/01/2019	0,528	20214,292	Not impulsive	S2	Intermediate soils
37	MOQ UNAM D845	ALGARROBAL	24/01/2019	0,113	18592,178	Not impulsive	S0	Hard rock
38	PALPA ICA D8D2	ANCASH SANTA	24/01/2019	0,305	25546,627	Not impulsive	S1	Rigid soils
39	TACNA 2010 TAC002	ALBERTO GIESEKKE MATTO	05/05/2010	0,272	64,598	Not impulsive	S0	Hard rock
40	LIM 001 2011	JORGE ALVA HURTADO	24/08/2011	0,057	702,340	Not impulsive	S0	Hard rock
41	LIM UNI 2011	DEPT ACADEM ESTRUCT	24/08/2011	0,311	284,350	Not impulsive	S1	Rigid soils
42	LIM 007 2001	VILLA EL SALVADOR	24/08/2011	0,510	62,859	Not impulsive	S2	Intermediate soils
43	LIM UNI2 2012	FIGMM UNI	30/06/2012	0,233	352,759	Not impulsive	S0	Hard rock
44	LIM 001 2012	JORGE ALVA HURTADO	30/01/2012	0,284	553,313	Not impulsive	S0	Hard rock
45	LIM 005 2012	PARQUE DE LA RESERVA	10/11/2012	0,144	1819,653	Not impulsive	S0	Hard rock
46	LIM 006 2012	PUENTE PIEDRA	10/11/2012	0,256	953,731	Not impulsive	S0	Hard rock
47	LIM 007 2012	VILLA EL SALVADOR	10/11/2012	0,144	722,144	Not impulsive	S0	Hard rock
48	LIM 005 2012	PARQUE DE LA RESERVA	02/08/2012	0,100	1478,922	Not impulsive	S0	Hard rock
49	LIM 006 2012	PUENTE PIEDRA	02/08/2012	0,226	951,456	Not impulsive	S0	Hard rock
50	LIM 008 2012	BOMBEROS 65 SMP	02/08/2012	0,256	670,159	Not impulsive	S0	Hard rock
51	TAC 002 2012	ALBERTO GIESEKKE MATTO	14/05/2012	0,456	69,517	Not impulsive	S2	Intermediate soils
52	TACNA TAC 002	ALBERTO GIESEKKE MATTO	07/06/2012	0,368	529,889	Not impulsive	S1	Rigid soils
53	LIM 002 2013	DECANATO FIC UNI	25/09/2013	0,172	989,585	Not impulsive	S0	Hard rock
54	LIM SLP 2013	CERRO UNI	25/09/2013	0,113	1090,062	Not impulsive	S0	Hard rock
55	LIM SLP 2014	CERRO UNI	15/03/2014	0,408	1064,678	Not impulsive	S2	Intermediate soils
56	LIM 001 2014	JORGE ALVA HURTADO	15/03/2014	0,291	1399,456	Not impulsive	S0	Hard rock
57	TAC 004 2015	SENCICO TACNA	11/02/2015	0,396	1116,573	Not impulsive	S1	Rigid soils
58	TAC 002 2015	ALBERTO GIESEKKE MATTO	11/02/2015	0,328	788,093	Not impulsive	S1	Rigid soils
59	TAC 001 2015	JORGE BASADRE	22/03/2015	0,224	257,917	Not impulsive	S0	Hard rock
60	TAC 004 2015	SENCICO TACNA	22/03/2015	0,523	238,757	Not impulsive	S2	Intermediate soils
61	TAC 003 2015	MUNICIPALIDAD CIUDAD NUEVA	22/03/2015	0,374	214,055	Not impulsive	S1	Rigid soils
62	TAC 002 2015	ALBERTO GIESEKKE MATTO	22/03/2015	0,439	212,177	Not impulsive	S2	Intermediate soils
63	LIMA UNI4 2011	LABORATORIO HIDRAULICA	24/08/2011	0,144	285,325	Not impulsive	S0	Hard rock
64	LIMA 002 2012	DECANATO FIC UNI	30/01/2012	0,156	1335,125	Not impulsive	S0	Hard rock
65	LIMA 0012012	DECANATO FIC UNI	30/01/2012	0,146	1503,677	Not impulsive	S0	Hard rock
66	LIMA 001 2012	BOMBEROS 65 SMP	30/01/2012	0,128	490,268	Not impulsive	S0	Hard rock
67	PRQUE RESERVA 1974	PARQUE DE LA RESERVA	05/01/1974	0,156	123,507	Not impulsive	S0	Hard rock
68	TACNA TAC001	JORGE BASADRE	13/06/2005	0,141	196,126	Not impulsive	S0	Hard rock

The signals were measured in seismic zone 4 of the Seismic Zoning Map, of the Peruvian Seismic Resistant Standard E.0.30, which corresponds to the region of the Coast of Peru. Zone 4 is where the epicenters of the most severe earthquakes that have occurred in the last 100 years have been located and in which a maximum horizontal acceleration on rigid ground of 0.45 is considered.

4. Inelastic Spectrum

4.1 Inelastic Input Energy Spectrum

For each Soil profile located in Seismic Zone 4 [3], the figures of inelastic Input Energy spectrum were prepared for structural behavior according to the structural perfect elastoplastic model.
Given the dispersion of data in each figure, the average curve and the average curve plus the standard deviation were plotted. As can be seen, the data dispersion is high, therefore, the standard deviation was greater than the average. Also, the maximum equivalent speed value was within a range of short periods between 0 and 0.5s. Likewise, the soil profile S1 is the one that reached the highest energy levels, with an equivalent speed that becomes 5 and 8 times the maximum equivalent speed of the soils with profile S0 and S1 respectively.

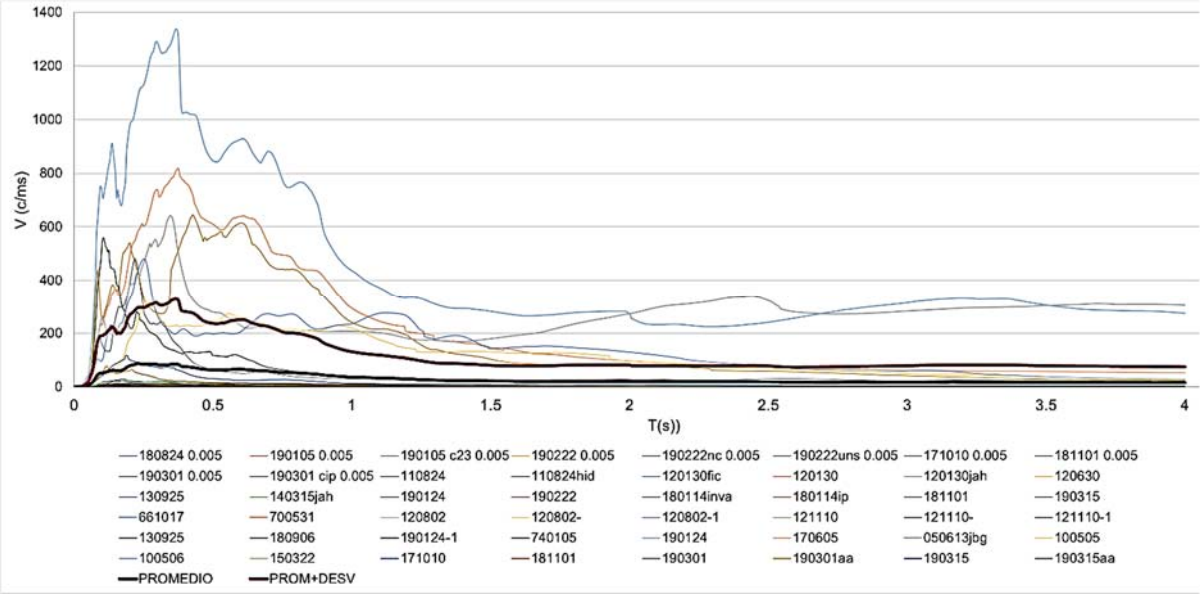

Fig.1: Input Energy Spectrum, Soil Type S0: Hard Rock

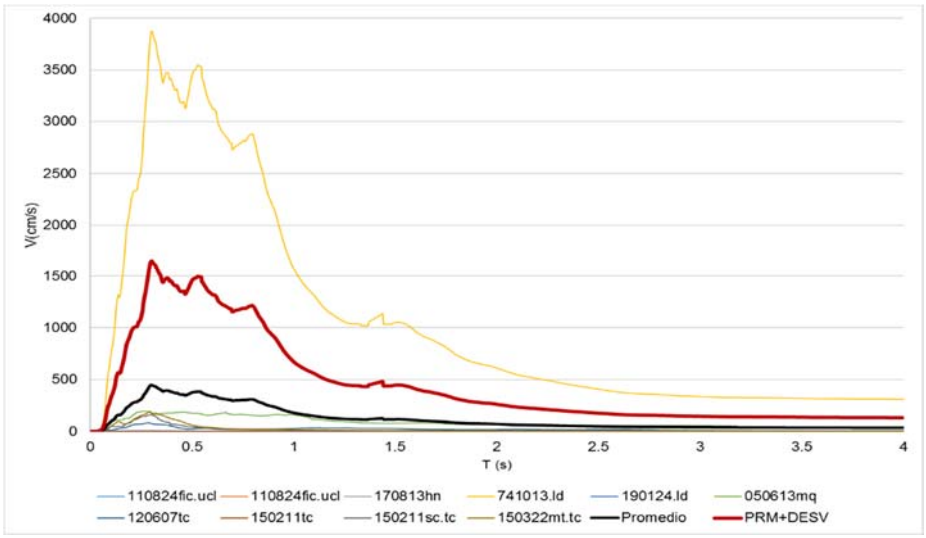

Fig.2: Energy Input Spectrum, Soil Type S1: Rigid Soils

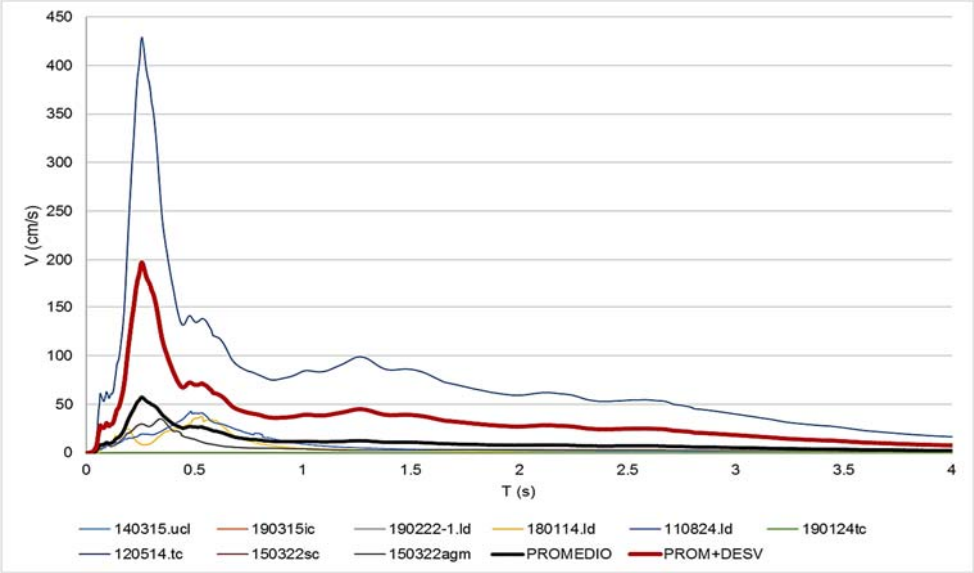

Fig. 3: Input Energy Spectrum, Type of Soil S2: Intemediate Soils

4.2 Inelastic Hysterical Energy Spectrum

The figures corresponding to the hysteretic energy spectrrum, specifically an important fraction of the input energy. This fraction is the energy dissipated by plastic deformation during the charge and discharge cycles. The perfect elastoplastic structural behavior is considered for the calculation and elaboration of these figures.

It is important to know that energy reduction factors produce inelastic energy spectrum that reasonably disperse the energy content of the "narrow band" movements of the soil, and produce a better characterization of inelastic energy demands according to Quinde [10].

Similar to the previous case, given the dispersion of data in each figure, the average was drawn and also the curve resulting from adding the average standard deviation. And similar from the input spectrum, there is a large dispersion of data, and that is the reason why the standard deviation standard is greater than the average.

Also, the maximum equivalent speed value was within a range of short intervals between 0s and 0.5s. On the other hand, it can be seen that the soil profile S1 is that the highest energy levels, with an equivalent speed that became approximately 5 and 8 times the maximum equivalent speed of soils with profile S0 and S1 respectively.

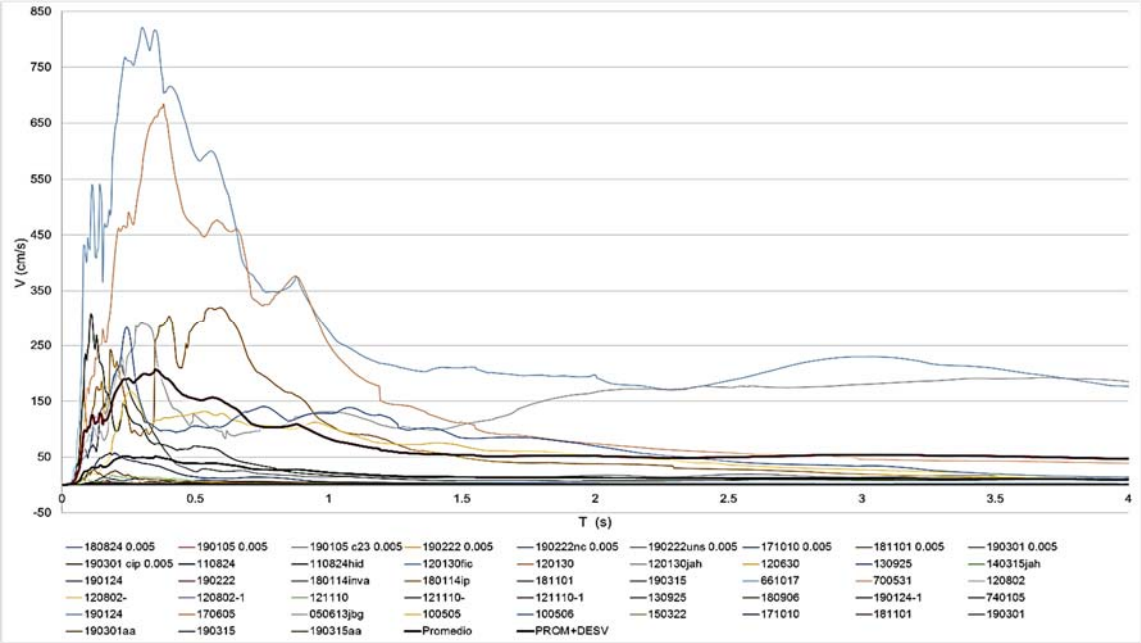

Fig. 4: Hysteretic Energy Spectrum, Soil Type S0: Hard Rock

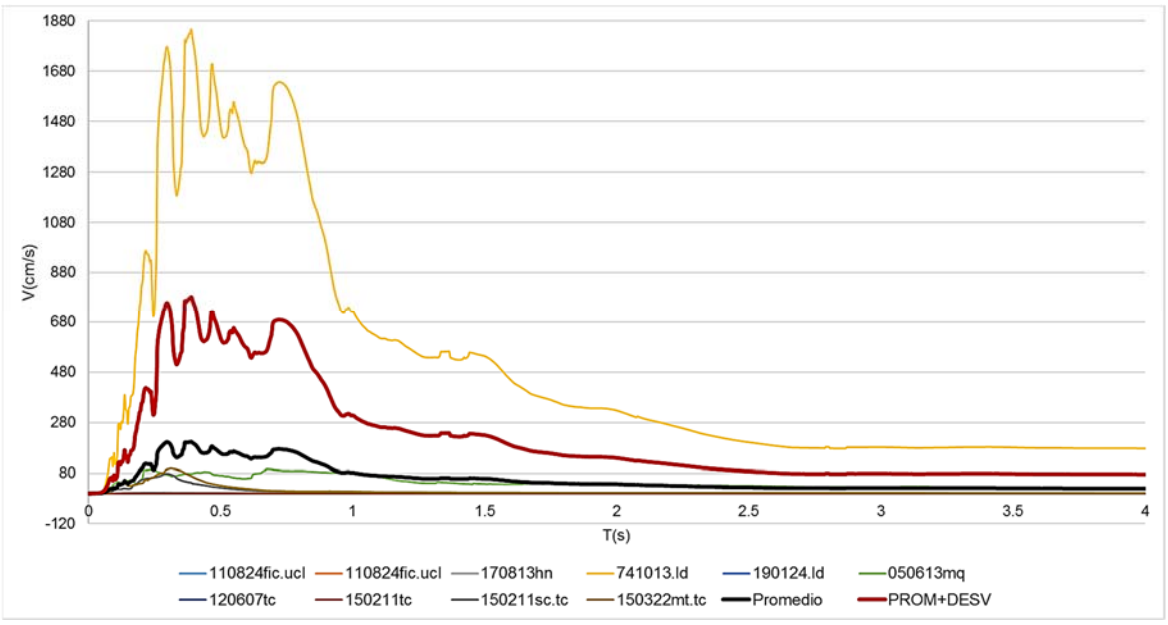

Fig. 5: Hysteretic Spectrum, Soil Type S1: Rigid Soils

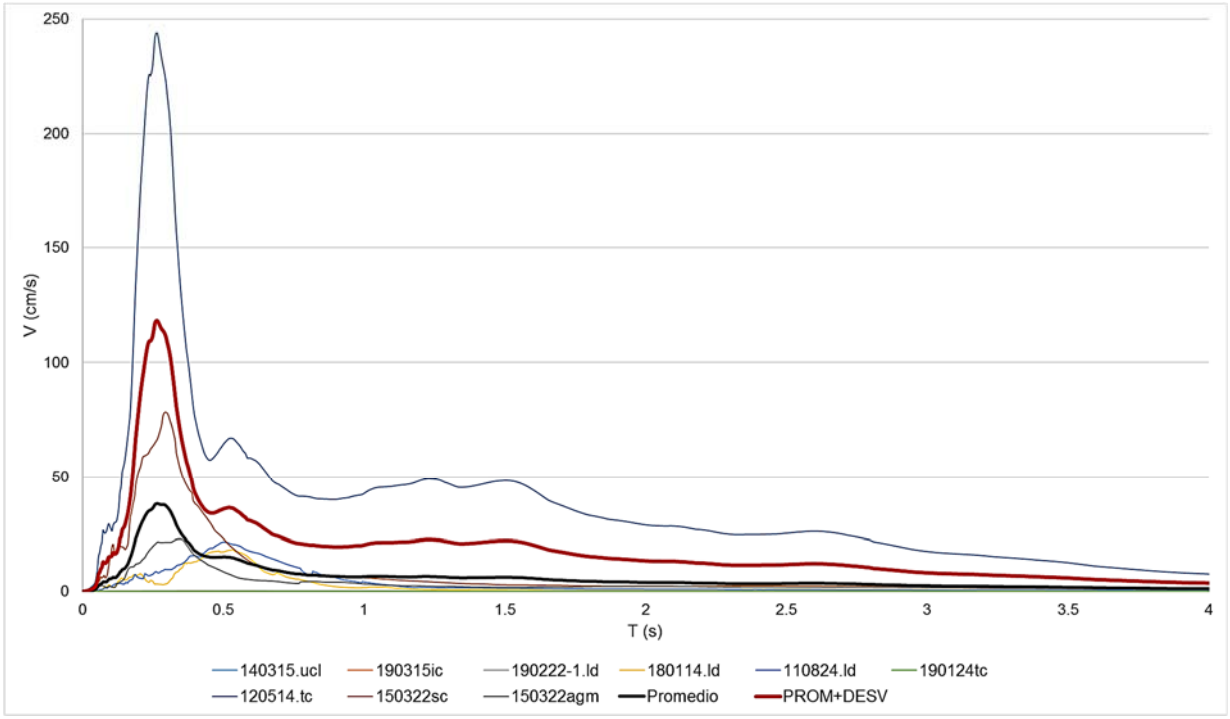

Fig. 6: Hysteretic Energy Spectrum, Type of Soil S2: Intemediate Soils

4.3. Input and Hysteria Energy Spectrum

This section shows the comparison of the average inelastic spectra of each soil profile. In this way you can see the fraction of the input energy that represents the hysteretic energy with respect to the input energy for each soil profile according to the current seismic-resistant design standard.

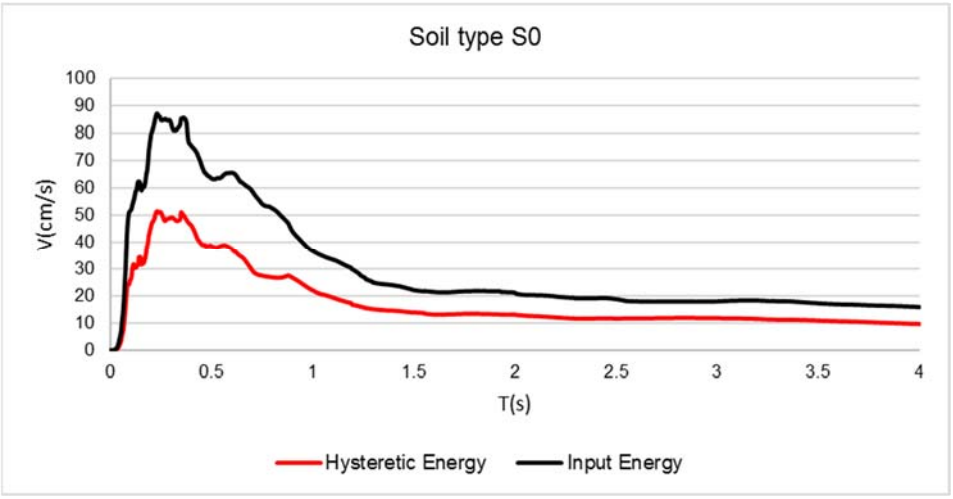

Fig. 7: Input and Hysteretic Energy for Profile S0

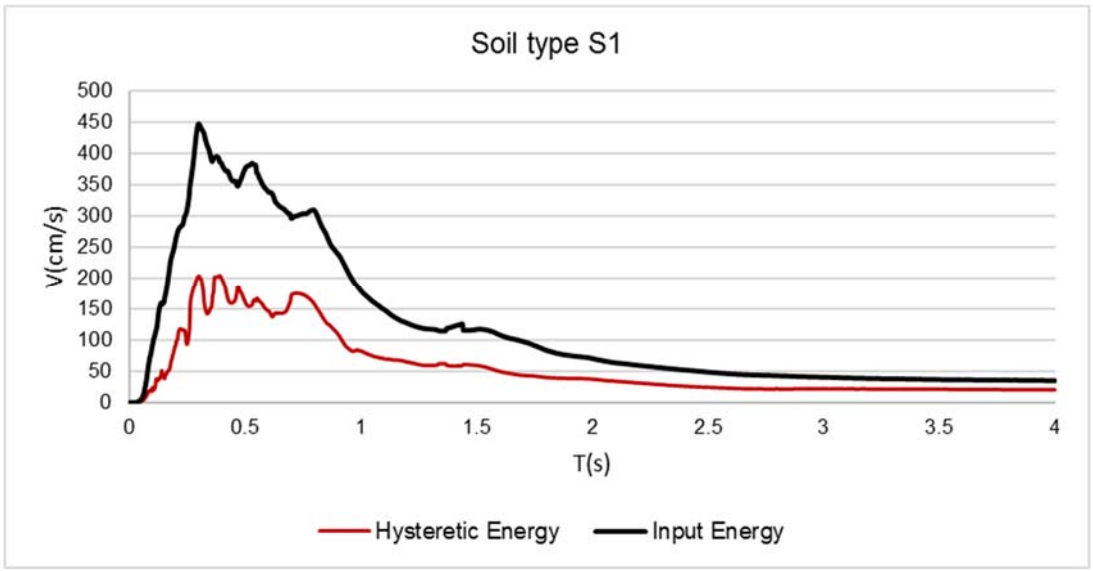

Fig. 8: Input and Hysteretic Energy for Profile S1

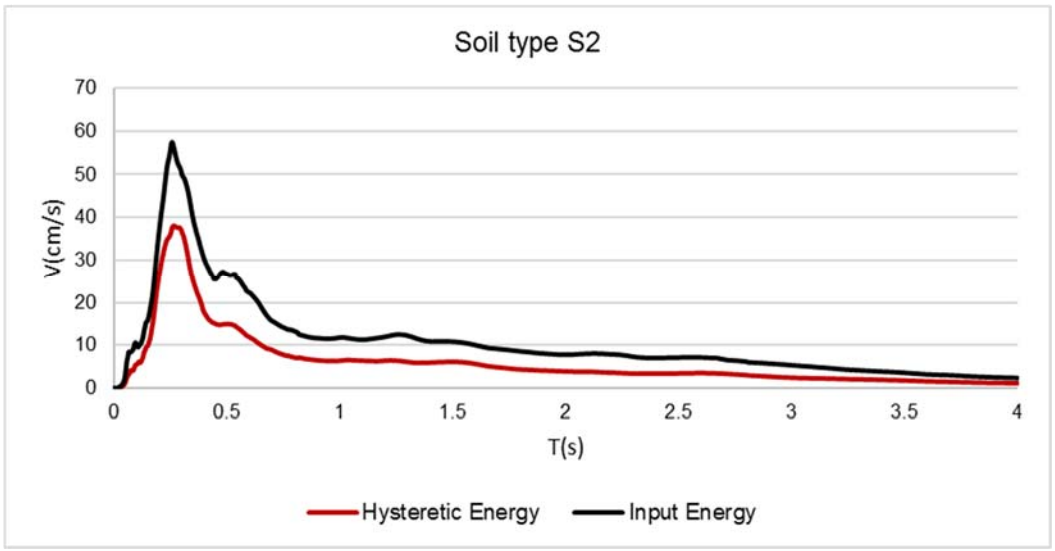

Fig. 9: Input and Hysteretic Energy for Profile S2

In Figs. 7 to 9 it is observed that the range of periods where the maximum energy dissipation is calculated is from 0.3s to 0.5 s. Also, on the point of maximum energy, the ratio of input energy to hysteretic energy is

approximately 0.5. In other words, in the period in which the increase in input energy reaches the maximum, it is recorded that about 50% of this energy is dissipated as hysteretic energy.

It is also appreciated that for rigid soils the maximum energy point (per unit mass), the average curve reached a value of 450 cm / s, which becomes nearly 5 and 8 times, respectively, the maximum energy level of entrance that for hard rock soils (S0) of 85 cm/s, or intermediate soils (S2) of 58 cm / s.

5. Conclusions

Given the current need to use energy concepts that take into account site conditions, soil types, earthquake intensity, and structural properties, inelastic energy spectra were developed using Peruvian earthquake records. Thus, from the inelastic spectra generated, the main conclusions are the following:

i) The hysteretic energy absorbed in the range of short vibration periods (T <0.5s), is approximately 50% of the input energy. Also, in rigid soils (profile S1) there are higher levels of energy absorption compared to hard or intermediate rock soils (profiles S0 and S2 respectively).

ii) Considering that, in Rigid Soils (S1), the level of plasticization and probable accumulated average damage to which the structures are exposed, will be considerably higher compared to hard or intermediate rock soils (in an order that exceeds 100%) it will be necessary to establish higher levels of ductility for the design of structures in the type of soil S1, in the range of short periods (T <0.5s).

iii) The use of severe earthquake signals, which were used to update the current E030 earthquake resistant design standard code [3], has determined the shape, and the maximum values reached by the average curves (including the standard deviation) of the inelastic spectra (input and hysteretic energy) therefore, it is inferred that the use of this standard code takes safety into account and is effective for damage control.

6. Acknowledgments

The authors would like to thank Dr. Mario Ordaz (UNAM) for his kindness in providing the Degtra 10.4 Software, and the Dr. (c) Arnold Mendo for providing some seismic records used in this work.

7. Copyrights

8. References

[1] Akiyama, H. (2003) “Methodology of the earthquake-resistant building project, based on the energy balance”. Spain: Editorial Reverte.

[2] Avendaño, J., Fernandez-Davila, V. I. (2014) “Enforcement the Design Method Based in the Energy Balance to Calculate Energy Spectra” Tenth U.S. National Conference on Earthquake Engineering – 10ncee

[3] Peruvian Standard for Seismic Resistant Design E030, updated to (2018)

[4] Choquehuanca, M. (2020). “Generation of Hysteretic Energy Spectra from a set of Peruvian seismic records”. Master thesis in Civil Engineering (In progress). Pontificia Universidad Católica del Perú.

[5] Bojorquez, E., Teran, A. (2009) “Explicit consideration of the accumulated damage in the seismic design of structures through ductility resistance reduction factors”. Seismic Engineering Magazine N°8031-62 (pag 31-55).

[6] Ordaz, M. (2018) Degtra 10.4. software, http://www.unam.me/news-unam/42-news-unam/21587-free-degtra-unam-mexico-download-degtra-unam-mexico-files.html.

[7] Seismosoft (2018). Seismosignal. Free trial. https://seismosoft.com/product/seismosignal/

[8] Hidalgo, D. (2017). "Probabilistic structural analysis aimed at assessing seismic damage with applications to construction typologies used in Costa Rica," Doctoral Thesis. Barcelona: Universidad Politécnica de Cataluña.

[9] Panella, S., Tornello, M., Frau, C. (2017). "A simple and intuitive procedure to identify pulse-like ground motions". Soil Dynamics and Earthquake Engineering. 94. 234-243. 10.1016/j.soildyn.2017.01.020.

[10] Quinde, P., Reinoso, E., & Terán-Gilmore, A. (2016). Inelastic seismic energy spectra for soft soils: Application to Mexico City. Soil Dynamics and Earthquake Engineering, 89, 198-207. https://doi.org/10.1016/j.soildyn.2016.08.004

